Observation of Muon Pairs in High-Energy Hadron Collisions*

J. H. Christenson,† G. S. Hicks,‡ L. M. Lederman, P. J. Limon, and B. G. Pope§
Columbia University, New York, New York 10027
and Brookhaven National Laboratory, Upton, New York 11973

E. Zavattini
CERN Laboratory, Geneva, Switzerland
(Received 30 March 1973)

Muon pairs with effective masses between 1 GeV/c^2 and 6.5 GeV/c^2 have been observed in the collisions of 30-GeV protons with a uranium target. The production cross section was seen to vary smoothly with mass exhibiting no resonant structure. Data were taken at incident proton energies of 22, 25, 28.5, and 29.5 GeV. Within the experimental aperture the total cross section increased with energy by a factor of 5. The experimental results are compared with the predictions of several theoretical models. Limits are presented for the contributions to the signal from both massive muon-pair resonances and antiproton-proton annihilation. Implications are presented for higher-energy accelerators, using current ideas involving scaling.

I. INTRODUCTION

We present here the results of an experimental study of the reaction

$$p + \text{uranium} \rightarrow \mu^+ + \mu^- + \text{anything} \qquad (1)$$

carried out at the Brookhaven AGS.[1] We measure the vector momentum of each of the muons emerging from the collisions of high-energy protons with a uranium target. Distributions are obtained of the effective mass, longitudinal momentum, transverse momentum, and polar angle of the muon pair.

The present research is an attempt to observe processes involving large momentum transfers and consequently contributing an infinitesimal fraction ($\ll 10^{-10}$) to the total cross section. The pair of muons is considered as a small-distance probe of the high-energy interaction volume, sensitive to structures which may be very weakly coupled to the $\mu^+\mu^-$ system. Reaction (1) is conventionally most relevant to studies of the electromagnetic structure of hadrons. The use of the AGS slow external proton beam and the choice of muons as the final-state particles enabled us to observe cross sections down to ~10^{-38} cm^2.

This subject has been investigated by a wide variety of techniques. Most notable has been the systematic study of the elastic electron-nucleon scattering form factors carried out by Hofstadter *et al.*[2] and by Wilson.[3] In elastic electron-proton scattering the square of the momentum transfer to the nucleon, q^2, is given by $q^2 \equiv -(\Delta E^2 - \Delta P^2) > 0$, the so-called spacelike region of momentum transfers. The form factors observed in these experiments decrease with increasing momentum transfer up to the highest values yet measured [$q^2 = 25$ (GeV/c)^2].[4] Theoretical considerations of the spacelike form factors have led to the ideas of vector dominance and to the prediction of isovector and isoscalar vector mesons with the same quantum numbers as the photon.[5,6] These known resonances do not fully account for the observed behavior of the nuclear form factors, and further, more massive resonances have been postulated.[7] Heavy vector mesons would modify the contributions of the known vector mesons only slightly in the spacelike region, while their effects could be seen directly as enhancements of the dimuon continuum when the effective mass of the muon pair is equal to that of the hypothetical vector meson (the timelike region, $q^2 < 0$).

Recent investigations of inelastic lepton-nucleon scattering[8] have once again indicated the extent to which a study of the electromagnetic form factors of hadrons may lead to further knowledge of such fundamental issues as the existence of elementary constituents of hadrons (quarks, partons, etc.). In this type of inclusive process[9] there is also a need to investigate the behavior for timelike momentum transfers in order to examine, and possibly extend, the conclusions of the scattering experiments. Exploration in the region of timelike photons then permits a search for possible resonances, and an investigation of the nature of any continuum.

There are several processes which involve timelike virtual photons. These have been studied from various aspects. In particular, much attention has been paid to the investigation of the validity of quantum electrodynamics (QED) in the timelike region. Here, experimental approaches have included colliding electron-positron beams,[10] muoproduction or electroproduction of lepton pairs,[11,12]

and measurement of $g-2$ for muons and electrons.[13] Photoproduction of the known vector mesons and examination of their relative couplings into pions, muons, and electrons can also be interpreted as a study of the photon propagator in the timelike region.[14] Similar interpretations can be drawn from the production of resonances in colliding electron-positron experiments.[15] There have been several photoproduction searches for higher-mass mesons that couple to lepton pairs.[16] As yet, these investigations have failed to find any such massive vector meson. In all of the above cases, the domain of sensitivity has been limited to momentum transfers ≤ 2 $(\mathrm{GeV}/c)^2$.

A direct measurement of the elastic electromagnetic form factors of the proton for timelike momentum transfers has been attempted by studying proton-antiproton annihilation into lepton pairs.[17] Only an upper limit for this annihilation mode was obtained $[\sigma_{\bar{p}p\to\bar{l}l} \leq 0.5$ nb for $q^2 = -6.8$ $(\mathrm{GeV}/c)^2]$. Finally, the e^+e^- annihilation into hadrons[18] is a powerful probe and seems to give results which are at variance with the simple parton model deduced from ep scattering.

A lepton pair production process,

$$A + B \to l^+ + l^- + C + D + \cdots , \tag{2}$$

where $A, B, C, D, \ldots$ are hadrons, measures the matrix element $\langle C, D, \ldots | J_\mu | A, B \rangle$, where J_μ is the hadronic part of the electromagnetic current operator, and the virtual photon associated with the current is timelike. To the lowest order in α, the fine-structure constant, lepton pairs serve to project out of the strong interactions those objects which have the same quantum numbers as the photon, i.e., the $J^P = 1^-$ vector mesons. Three experiments employing negative pions as an incident particle have succeeded in observing the spectrum of muon pairs up to an effective mass of $\simeq 1$ GeV/c^2, and the resonant contribution of the ρ^0 meson was clearly seen.[19-21]

The present experiment observed muon pairs produced in the collisions of high-energy ($\approx$30 GeV) protons with uranium. The effective mass of the muon pair ($M_{\mu\mu}$, the relevant variable in the timelike region) was calculated from the momenta (p_1, p_2) and angles (θ_1, θ_2) of the observed muons via

$$M_{\mu\mu}{}^2 = 2p_1 p_2 [1 - \cos(\theta_1 + \theta_2)] . \tag{3}$$

The high energy and intensity of the extracted proton beam at the AGS permitted the observation of effective masses as high as 6.5 GeV/c^2 [$q^2 = -M_{\mu\mu}{}^2 \approx -40$ GeV/c^2] where the collision probability is 10^{-13} of the total hadronic cross sections.

The study of muon pairs in this case was facilitated by the fact that the overwhelming strongly interacting background could be largely suppressed by absorption in the dense uranium target (interaction length $\approx$11 cm). Thus, in particular, most pions interacted before they could decay into muons (decay mean free path $\approx$550 m for a 10-GeV pion).

The experimental results show a smooth, steeply falling continuum as a function of the invariant mass of the muon pair with no convincing evidence for any resonant structure. A description of the experimental method and the analysis of the data follow.

II. EXPERIMENTAL METHOD

A. Absorbers and Detectors

The slow extracted proton beam of the Brookhaven AGS was transported in vacuum to a uranium target consisting of 20 1-in. plates which were ar-

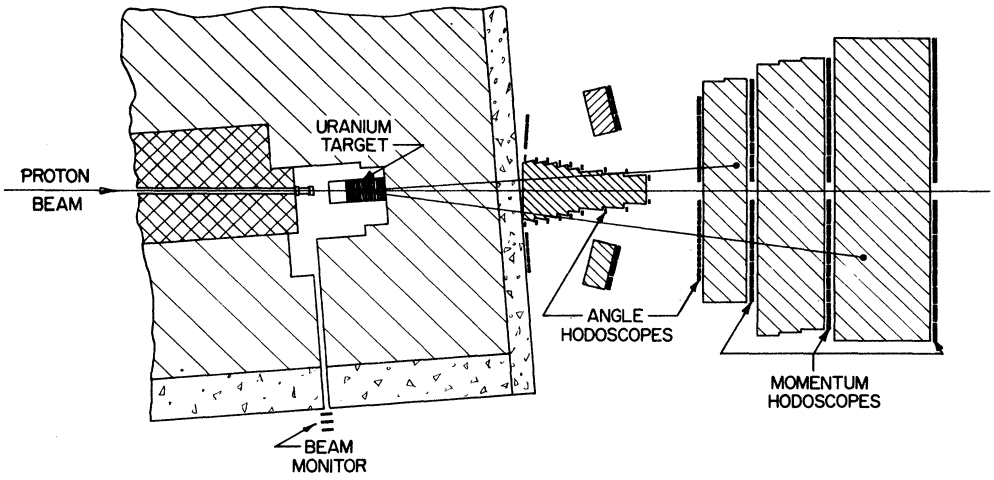

FIG. 1. Plan view of apparatus.

ranged in accordion fashion to enable the effective density of the target to be varied by as much as a factor of 3. The dense target served to suppress the large background flux of strongly interacting particles and, in particular, to absorb most pions and kaons before they decayed. Immediately behind the target was a 10-ft-thick steel wall, followed by a 2-ft wall of heavy concrete (see Fig. 1). These absorbers provided a momentum threshold of 6 GeV/c and thus acted to discriminate against muons from those pions or kaons that did decay. An additional absorber was supplied by a wedge-shaped steel block that varied in thickness in the beam direction from 11 ft for the smallest muon angle accepted (40 mrad) to 0 for the largest angle (250 mrad). This absorber constrained the transverse momentum of a detected muon to exceed 450 MeV/c, resulting in further discrimination against muons from pions or kaons without seriously affecting the detection efficiency for high-mass muon pairs.

Multiple scattering in the steel and concrete absorbers produced an uncertainty that precluded any precise measurement of the emerging muon angle. A measurement of the emergent position of the muon using a counter hodoscope was considered adequate. This angular uncertainty, in turn, limited the mass resolution to the extent that the initial momentum of each muon could be calculated well enough from a fairly crude measurement of its range in steel.

Particles emerging from the wedge-shaped absorber were recorded by a 36-element solid scintillation-counter hodoscope mounted on the insets of the tapered wedge. There were two counters, each 4.5 in. wide by 8.6 in. high, on each inset of the wedge; one above beam height and one below. There were 9 insets (18 counters) on each side of the extrapolated proton beam line. This hodoscope served to define the angle of each emergent muon; the origin of the muon was assumed to be in the uranium target. A subsequent plane of liquid scintillators provided an angular confirmation that was sufficient to greatly reduce the sensitivity to extra-target muon production. Additional planes, following 4-, 6-, and $8\frac{1}{2}$-ft-thick steel walls, were used to measure the range of each muon and hence its initial momentum.

At the highest incident proton energy at which data were recorded, 29.5 GeV, the first hodoscope was extended by the addition of two banks of solid counters outside the outermost counters of the standard configuration. Range information for muons passing through this outer detector was obtained from a plane of three liquid counters placed behind 24 in. of steel as shown in Fig. 1.

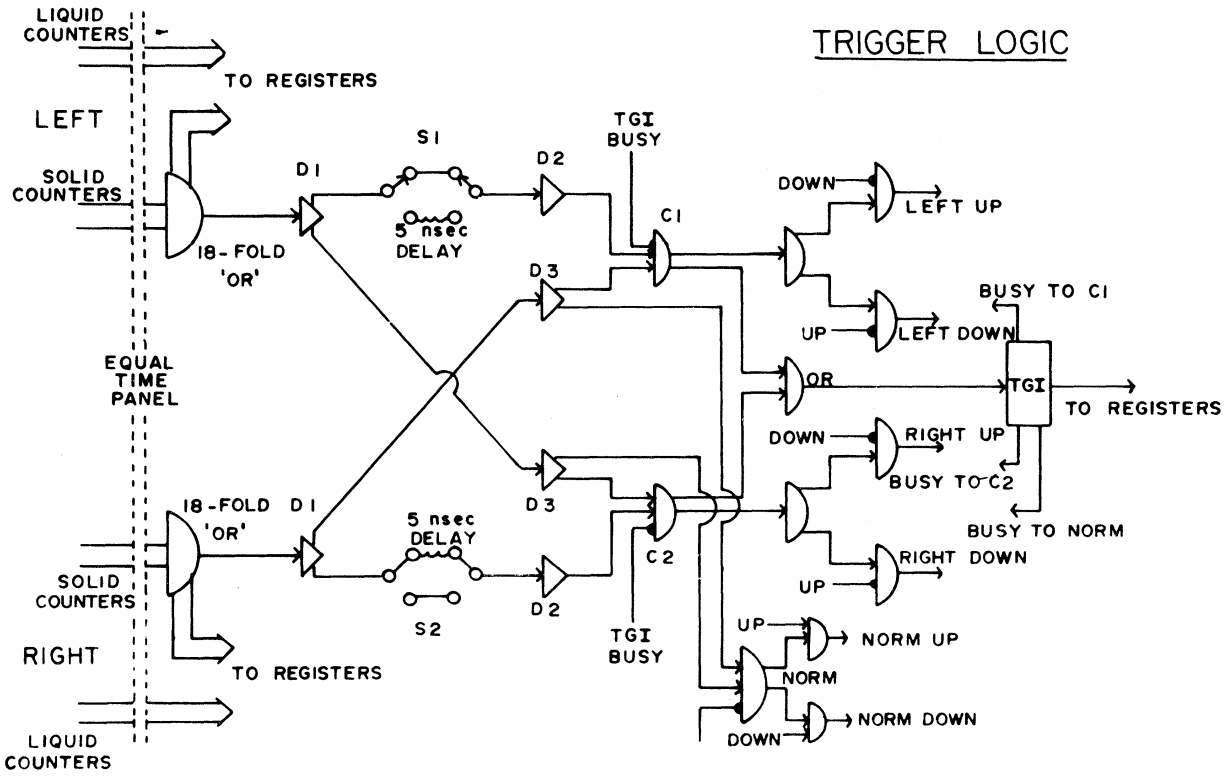

FIG. 2. Schematic diagram of trigger electronics.

B. Electronics

Muon pair candidates were characterized by a coincidence between the left and right halves of the first hodoscope. Typically 2.5×10^{11} protons were incident on the uranium target during a 300-msec spill each AGS pulse. Fluxes of approximately 10^6 muons/sec were observed in the first counter hodoscope. The resolving time of the coincidence circuit was 2.7 nsec [full width at half maximum (FWHM)] and so a large number (about 2000 per pulse) of accidental muon pairs were recorded. A continuous measurement was made of these accidental coincidences by using a separate coincidence circuit in the trigger logic. The electronics could be triggered either by a coincidence of simultaneous muons or by a coincidence of muons produced in the target 5 nsec apart. A schematic diagram of the trigger electronics is shown in Fig. 2. The former category (in-time coincidences) contained both real muon pairs and the dominant background of accidental coincidences. The latter category (delayed coincidences) contained only the background. Any real dimuon signal could then appear as the difference between the in-time coincidences and the delayed arm. Between AGS pulses, coaxial relays interchanged the roles of these two circuits, thereby canceling the error arising from slight differences in their resolving times. A third broad coincidence circuit monitored the accidental rate, pulse by pulse, for both relay positions and so permitted corrections due to fluctuations in beam intensity and duty cycle.

After the occurrence of either an in-time or a delayed coincidence, the trigger logic circuits were held in an off state for at least 200 nsec while an analysis of the triggering event was performed by a system of register logic. These circuits interrogated the status of each counter in the detector during the triggering event. Elementary requirements of quality and consistency were imposed upon each muon trajectory, and each trajectory was classified as to angle and range. For simplicity in analyzing events, no events were accepted in which more than one counter fired in each bank. A stipulation of continuous trajectories was also made, in which the first two planes were required to have counted. In the interrogation of each counter the time of the pulse from that counter with respect to the triggering time was also recorded. Prior calibration of each counter enabled an estimate of the vertical position of the muon at each plane to be made. Thus, further discriminations against both extratarget production and accidental extension of the trajectory could be made.

If the triggering event failed to meet the above requirements, the registers were cleared and the trigger logic again activated in order to receive the next coincidence. In the case of accepted events, however, the trigger logic was held off for a further 800 nsec to permit the transfer of information on active counters to a data formatter. The data formatter assembled the information into 36-bit words, in which form it was transferred to a data handler that could store up to 4000 words (approximately 1200 events). Between each machine pulse the contents of the data handler were transmitted to the Brookhaven PDP-6 computer for analysis and storage. Simultaneously, it was possible to write a tape record of the raw information of each event.

Additional data that were also read into the computer included information from counters measuring the intensity and quality of each machine pulse. An on-line analysis program monitored all counter rates in the experiment and performed logical checks on 10–15% of the data.

An equally important function of the on-line program was condensing the data to a manageable form. In the course of the experiment, more than 300 million events were recorded. These events came in at the rate of about 2000 per machine cycle. All the data for each event could not be stored conveniently. Consequently, only a fraction ($\sim\frac{1}{8}$) of the raw data were directly recorded. The software, on the other hand, examined *all* the events, extrapolated all trajectories back to the target, checked for accidental trajectories, and compiled all good events in a 3412-word master event histogram representing the possible combinations of counter firings and trigger circuit configurations. In addition, the on-line program summarized the data accumulated during each one-hour run and produced a listing of pertinent information for later reference.

Due to the high single-muon rate, most of the 300 million events that were recorded were un-

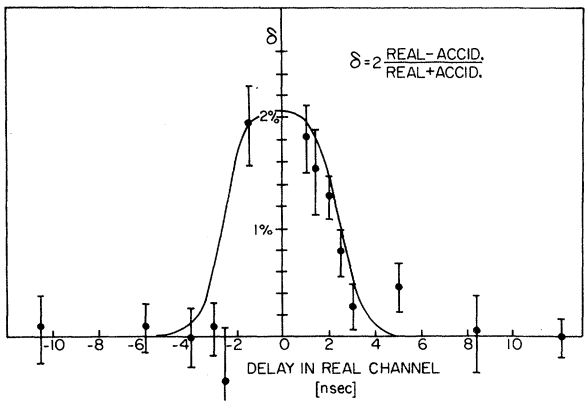

FIG. 3. Delay curve showing real dimuon effect.

wanted accidentals. However, for each of the four incident proton energies at which data were taken, a small real dimuon effect was observed. This real effect is illustrated as a function of delay in the "in-time" channel in Fig. 3. Computer information on the vector momentum of each of the two muons enabled the calculation of various kinematical quantities of the dimuon system, such as mass [$M_{\mu\mu}$ given by Eq. (3)], laboratory momentum ($\vec{p}_{\mu\mu}=\vec{p}_1+\vec{p}_2$), and laboratory angle [$\theta_{\mu\mu}=(\vec{p}_1\cdot\vec{p}_2)/|\vec{p}_1||\vec{p}_2|$]. The real signal for an incident energy of 29.5 GeV is displayed as a function of the effective mass of the muon pair in Fig. 4.

III. DATA ANALYSIS

A. Verification of a Dimuon Signal

1. Reality of the Effect

The real dimuon spectra, obtained as the difference between the numbers of in-time and delayed coincidences and shown in Fig. 4, amounted to some 4% of the in-time data sample. The real effect varied with dimuon mass from 2% at 1.5 GeV/c^2 to 40% at 5 GeV/c^2. As seen in Fig. 4 the events appear as a broad continuum, extending over the entire mass aperture of the experiment.

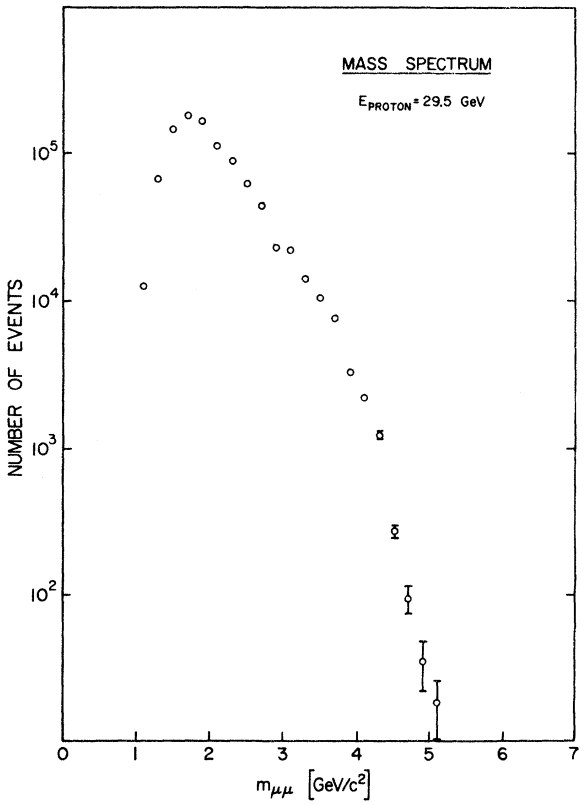

FIG. 4. Observed events as a function of the effective mass of the muon pair. Proton energy=29.5 GeV.

Of course, with such a small signal-to-noise ratio, the data were extremely sensitive to systematic effects that would distort the subtraction procedure. Exhaustive tests were performed to ensure that no such distortion was present.

The symmetry of the two coincidence circuits was checked and adjusted using a large number of radioactive sources placed near to the trigger counters to supply a signal that manifestly had no time correlation (or real signal). It was found that the numbers of coincidences recorded in the two circuits were always the same to within 0.03%. A more extensive test of this symmetry and the effectiveness of the switching technique was carried out by operating both circuits with a relative delay of 5 nsec inserted. Thus, both circuits should have recorded only the background of "accidental" coincidences. Data were taken in an otherwise normal manner and the test clearly probed for biases in the trigger and register logic as well as in the data handler and computer. The real, or subtracted, signal produced by this test was consistent with a null result ($\chi^2=18$ for 20 degrees of freedom) with no suggestion of a mass bias in the procedure. The total numbers of events in the two channels were the same to within 0.3%, yielding an uncertainty of $7\frac{1}{2}$% of the real signal due to coincidence circuit or subtraction asymmetries. The choice of an uncertainty of this amount rather than the value obtained from the radioactive-source runs (a factor of 10 smaller) is conservative and is motivated by the possibility of subtle effects in the actual data. By its nature, the background of accidental coincidences varied as the square of the intensity of the primary proton beam. Lack of systematic variation of the real muon-pair cross section with proton intensity is further evidence that the real signal cannot be attributed to accidental coincidences.

Another potential source of a spurious dimuon signal was radio frequency structure in the primary proton beam. This would cause a difference in the single-muon flux (and hence the accidental coincidence rate) between the "in-time" coincidence arm and the "delayed" arm. Normally high-frequency time structure introduced by the AGS acceleration process (peak-to-peak time characteristically[22] 220 nsec) was effectively removed in the extraction process of the external beam. Operating the beam with deliberate rf structure enabled a study of this effect to be made, and during these studies a monitoring procedure was developed. Accidental coincidence rates for relative delays of 0 nsec (peak) and 110 nsec (valley) were compared. The difference between these two readings measured the fractional effect of the rf oscillations. This signal was recorded by the on-line computer

and was also monitored in the AGS control room. Under normal operating conditions, the amplitude of rf structure was <10%, and thus for a delay time 5 nsec rf effects would contribute negligibly to a real dimuon signal.

Another effect of beam time structure that could simulate a real signal arises from statistical fluctuations in the intensity of the primary proton beam. These fluctuations would produce a correlation in the single-muon fluxes observed in the apparatus. This correlation would, of course, affect only the "in-time" circuit. The effect was estimated to contribute, at most, about 2.5% of the real dimuon signal.

2. *Spurious Sources of a Real Effect*

Having established the viability of the subtraction procedure, we now examine various sources of a real effect.

a. Upstream sources. Interactions of the primary proton beam with material upstream of the uranium target could have resulted in the creation of muon pairs (probably from the double decay of pion pairs). Because of the assumption of target production, these dimuons would, in general, simulate a large-angle pair with a corresponding error in the calculated effective mass. Special runs to examine and estimate this source of error were made. In some runs, the proton beam was deliberately defocused so that a large fraction struck the walls of the vacuum pipe and the collimators. In other runs, material was inserted into the beam at various points. Preliminary tests indicated that the observed dimuon signal was indeed sensitive to these variations. As a result, the vacuum pipe was surrounded with closely packed lead for some 30 ft upstream of the target, as shown in Fig. 1. Further studies then showed that the dimuon signal was fully stable with respect to the artificial generation of upstream sources. Nevertheless, a two-counter telescope which looked upstream of the target was installed. This telescope was found to be extremely sensitive to upstream muon sources and it was monitored throughout the experiment.

b. Pionic sources. Pion (or kaon) pairs produced in the very dense target had a considerable likelihood ($10^8:1$) of interacting before decaying into muons. Nevertheless, the possibility that this source contributed to the real signal was examined. The accordionlike nature of the target permitted its effective density to be reduced by as much as a factor of 3. Special runs were made with the target length extended to 60 in., thus increasing the probability of a double pion decay by a factor of ~9. However, no change in the real signal was observed and a limit of 10% was placed on the possible contribution of pion pairs produced in the target.

B. Apparatus Detection Efficiency

The effect of the experimental apparatus on the muon pairs produced in the target is now considered. The geometry of the detectors and the absorbers placed strict momentum and angle limits on each muon. Many dimuons produced in the target were not detected; in order to calculate a cross section that is independent of these specific experimental conditions, corrections must be made for this fact. Many of the corrections involve detailed considerations of the passage of charged particles through the absorbers. Hence the size of the detectors and the momentum limits of the absorbers should be applied only after a study of phenomena such as multiple Coulomb scattering, ionization loss, and range straggling. For these corrections, an elaborate Monte Carlo simulation of the experiment was employed.

There were, however, some more easily calculable corrections that were applied to the data independently of the Monte Carlo program. Losses of events due to counter-bank inefficiencies or to accidental vetoing by an extraneous particle fall into this category. Corrections due to these effects were estimated from a special series of runs which measured the single-particle rates of each of the 130 counters and also investigated the number of events that were recorded for various configurations of the triggering requirements. In this way, the fraction of muon trajectories containing more than one counter in any particular bank was measured. Similarly, the rates of those trajectories that were incomplete, giving no count in an intermediate hodoscope, were also estimated. Timing losses, due to dead time in the coincidence and pulse-shaping circuits, were also corrected for at this time. The corrections resulting from the above effects increased the signal by a factor of 2 with very little change in the shape of the mass distribution of muon pairs.

The Monte Carlo program contained the exact geometry of the various absorbers and detectors in the experiment, together with the necessary information for describing the passage of charged particles through matter. The production of either single muons (from pion or kaon decay) or muon pairs could be simulated in the computer.

The interaction point distribution of the 30-GeV protons in the uranium was represented by an exponentially falling distribution, after a "transition region" of 5 in. (≈1 interaction length).[23] Muons were then propagated through the apparatus while

the effects of multiple Coulomb scattering,[24] ionization loss to the electrons in the absorbers,[25] and range straggling[26] were included. Muons were required to have sufficient initial momentum to emerge from the absorber, to pass through one counter in the first hodoscope, and then to hit the second hodoscope. The range of the muon, after straggling and subtracting the thickness of primary wall through which it had passed, determined in which range block it would stop. The apparent range and angle of each detected muon were recorded on magnetic tape. This information constituted the output of the Monte Carlo program.

An independent test of the Monte Carlo propagation of muons through the apparatus was provided by its ability to predict the spectrum of accidental coincidences observed in the experiment. A pion and kaon production spectrum was used as an input to the Monte Carlo program,[27] the pions and kaons were allowed to decay, and the resulting muons propagated through the apparatus. With experimental information on the coincidence resolving time and the duty factor of the beam, an accidental mass spectrum could be generated that contained no adjustable parameters. The experimental and the Monte Carlo distributions are compared in Fig. 5. While the predicted curve is seen to be narrower than the observed spectrum, the agreement is thought to be a satisfactory indication of the reliability of the Monte Carlo program. More detailed examination of the discrepancies between the Monte Carlo distribution and the data showed that the experimental distributions exceeded the predicted distributions for larger pion and kaon angles. Alternative pion production spectra[28] are, in fact, capable of supplying this needed excess at larger angles, and would thus produce better agreement between experiment and theory.

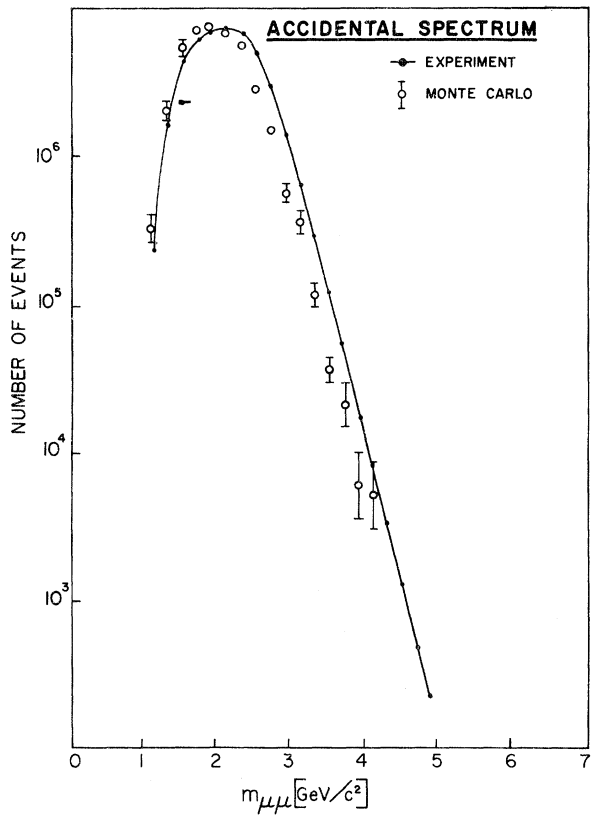

FIG. 5. The mass spectrum of "accidental" events compared with Monte Carlo predictions.

The mass resolution, due mainly to multiple scattering and the quantizing of the angle and momentum measurements, was determined by the Monte Carlo calculation to be ±12% at 2 GeV/c^2 and ±8% at 4 GeV/c^2. The determination of the detection efficiency of the apparatus as a function of mass was complicated by this mass smearing. This was particularly true for a signal that consisted of a fast-falling continuous distribution. Thus the efficiency and hence the measured cross section were dependent on the dimuon production models used in the Monte Carlo calculation. These models were, of course, the very quantities that this experiment sought to determine. This is always the penalty for exploring a totally new domain of physics with less than a 4π solid angle and less than a zero to infinity momentum aperture. A phenomenological theory was constructed using a small number of variable parameters specifying the dimuon system: its effective mass, longitudinal momentum, laboratory angle, and decay distribution into two muons. This model was then inserted into the Monte Carlo calculation and the parameters varied with the requirement that the output distributions of the computer simulation correspond to those of the observed data. As exact agreement with the data in all dimensions was extremely difficult, the "best" models were used to calculate an apparatus detection efficiency and those models that gave obviously poor fits were used to investigate the sensitivity of this efficiency to the model. The detection efficiency was then applied to the data to give the required cross sections. This procedure was adopted because it was found that the detection efficiency was fairly stable with respect to wide variation of parameters in the input model. Errors due to a slightly incorrect input function would then not cause substantial errors in the quoted cross sections.

Various dimuon-production models were examined. These models were required to be smooth and continuous [each dimension specified by a small number (≤ 3) of parameters]. In the dimension of invariant mass, this criterion represented a conclusion that the observed mass spectrum con-

tained no evidence of any resonant structure. (Investigations of the effects of resonant structure were carried out by the addition of a narrow enhancement to the smooth model, as discussed in the next section.) Simple correlations between the dimensions of mass, momentum, and angle were considered and found to be unnecessary. The distribution in θ_μ^*, the muon decay angle in the pair center of mass, was assumed to be isotropic. Poor resolution in θ_μ^* coupled with a limited aperture around 90° frustrated measurement of this distribution. Other possible distributions such as $\sin^2\theta_\mu^*$ or $1+\cos^2\theta_\mu^*$ do not alter the shapes of the observed cross sections but do change the normalization by ±20%.

For all models the kinematical constraints of three-body phase space were included. This would imply the simplest possible reaction:

$$p+N \rightarrow p+N+\text{“}\gamma\text{”} \searrow \mu^+ + \mu^- . \tag{4}$$

It was believed that this removal of kinematic effects from the trial model would supply essential physical restrictions and cutoffs and enable the cross sections to be described by a smaller number of parameters. Variations in the empirical model would correct for any divergence from the simple three-body final-state conditions.

The above procedure of finding a "best" model and then investigating large excursions about this distribution was performed for the data at all incident proton energies. It was deemed important that the "best" parameters should not vary wildly with this change in energy. Indeed, it was found that the parameters specifying the mass and angular distributions were unchanged and that the two parameters specifying the longitudinal momentum distribution changed only slightly and in a smooth fashion.

IV. RESULTS

A. Observation of a Continuum Distribution of Muon-Pair Masses

Production cross sections were calculated from data using

$$\sigma = \frac{(\text{data})\times(\text{total nucleon-nucleon inelastic cross section})}{(\text{number of protons})\times(\text{efficiency})} . \tag{5}$$

The cross sections were thus calculated per free target nucleon. The total nucleon-nucleon inelastic cross section was taken to be 20 mb.[29] In general, differential cross sections (e.g., $d\sigma/dq$, $q=M_{\mu\mu}$) were calculated, where the width of each interval was chosen to be less than the resolution width. The number of protons incident on the target was obtained using the beam monitor shown in Fig. 1. This counter telescope was calibrated using the secondary emission chamber (SEC) operated by the AGS slow external beam group.[22]

The differential cross sections as a function of the effective mass of the muon pair ($d\sigma/dq$) are given in Table I for all four proton energies at which data were taken. The statistical errors shown in Table I arise from both the data and the Monte Carlo calculation. These four differential cross sections are shown in Figs. 6–9. The cross section for an incident proton energy of 29.5 GeV may be roughly represented as

$$\frac{d\sigma}{dq} \approx \frac{10^{-32}}{q^5}\ \text{cm}^2/(\text{GeV}/c^2) .$$

The spectra at the other energies exhibit a similar mass dependence but a smaller total cross section. All cross sections quoted are restricted by the over-all "aperture" of the experiment and thus are given for masses greater than 1 GeV/c^2, for laboratory momenta above 12 GeV/c, and for production angles out to 65 mrad. These aperture limitations are clearly more severe for the lower-energy data.

The addition of the banks of counters at wide angles (Fig. 1) during runs made at an incident proton energy of 29.5 GeV enabled the range of the mass survey to be increased to $\simeq 7$ GeV/c^2. Figure 10 shows $d\sigma/dq$ for an energy of 29.5 GeV calculated on the basis of all counters. Table II tabulates this cross section with statistical errors and also gives the systematic errors arising from the input-model uncertainty. The systematic errors were estimated from the behavior of the efficiency under extreme variations of the input model. These errors are not independent of one another. Rather they collectively describe an envelope within which $d\sigma/dq$ may vary in a smooth manner. The increased mass range indicates a steeply falling cross section consistent with the rapid reduction of phase space. Fermi motion of the target nucleons provides sufficient center-of-mass energy to create muon pairs above the 5.7-GeV/c^2 kinematic limit.

Differential cross sections for the other variables used to specify the initial state of the dimuon system [the laboratory longitudinal momentum, p_L, and the cosine of the laboratory angle of the dimuon with respect to the proton beam direction ($\cos\theta$)] were obtained by a procedure that was in

TABLE I. $d\sigma/dm$ for four incident energies.

Mass (GeV/c^2)	$\frac{d\sigma}{dm}$ [$cm^2/(GeV/c^2)$] E_{proton} 29.5 GeV	28.5 GeV	25 GeV	22 GeV
1.1	$(1.61\pm0.4)\times10^{-32}$	$(1.18\pm0.3)\times10^{-32}$	$(0.479\pm0.15)\times10^{-32}$	$(1.49\pm1.2)\times10^{-32}$
1.3	$(4.37\pm0.5)\times10^{-33}$	$(3.35\pm0.4)\times10^{-33}$	$(1.21\pm0.2)\times10^{-33}$	$(1.59\pm0.6)\times10^{-33}$
1.5	$(1.80\pm0.2)\times10^{-33}$	$(1.55\pm0.1)\times10^{-33}$	$(0.661\pm0.07)\times10^{-33}$	$(0.402\pm0.09)\times10^{-33}$
1.7	$(8.38\pm0.7)\times10^{-34}$	$(7.07\pm0.6)\times10^{-34}$	$(3.15\pm0.3)\times10^{-34}$	$(1.30\pm0.3)\times10^{-34}$
1.9	$(4.81\pm0.2)\times10^{-34}$	$(4.25\pm0.2)\times10^{-34}$	$(1.98\pm0.1)\times10^{-34}$	$(1.07\pm0.1)\times10^{-34}$
2.1	$(2.66\pm0.1)\times10^{-34}$	$(2.52\pm0.1)\times10^{-34}$	$(1.22\pm0.09)\times10^{-34}$	$(0.612\pm0.09)\times10^{-34}$
2.3	$(1.69\pm0.08)\times10^{-34}$	$(1.73\pm0.08)\times10^{-34}$	$(0.825\pm0.05)\times10^{-34}$	$(0.416\pm0.06)\times10^{-34}$
2.5	$(1.14\pm0.05)\times10^{-34}$	$(1.11\pm0.06)\times10^{-34}$	$(0.538\pm0.04)\times10^{-34}$	$(0.317\pm0.04)\times10^{-34}$
2.7	$(7.19\pm0.3)\times10^{-35}$	$(7.47\pm0.3)\times10^{-35}$	$(3.70\pm0.3)\times10^{-35}$	$(1.50\pm0.3)\times10^{-35}$
2.9	$(5.45\pm0.3)\times10^{-35}$	$(5.11\pm0.3)\times10^{-35}$	$(2.64\pm0.3)\times10^{-35}$	$(1.37\pm0.3)\times10^{-35}$
3.1	$(4.53\pm0.2)\times10^{-35}$	$(4.25\pm0.2)\times10^{-35}$	$(1.49\pm0.2)\times10^{-35}$	$(0.940\pm0.17)\times10^{-35}$
3.3	$(4.77\pm0.2)\times10^{-35}$	$(4.11\pm0.2)\times10^{-35}$	$(1.72\pm0.2)\times10^{-35}$	$(0.414\pm0.18)\times10^{-35}$
3.5	$(4.28\pm0.2)\times10^{-35}$	$(3.28\pm0.2)\times10^{-35}$	$(1.14\pm0.1)\times10^{-35}$	$(0.385\pm0.15)\times10^{-35}$
3.7	$(3.78\pm0.2)\times10^{-35}$	$(3.06\pm0.2)\times10^{-35}$	$(1.11\pm0.1)\times10^{-35}$	$(0.413\pm0.12)\times10^{-35}$
3.9	$(3.37\pm0.2)\times10^{-35}$	$(2.46\pm0.1)\times10^{-35}$	$(1.17\pm0.1)\times10^{-35}$	$(1.77\pm0.5)\times10^{-35}$
4.1	$(2.70\pm0.1)\times10^{-35}$	$(2.31\pm0.1)\times10^{-35}$	$(0.893\pm0.1)\times10^{-35}$	$(0.724\pm0.4)\times10^{-35}$
4.3	$(1.57\pm0.1)\times10^{-35}$	$(1.30\pm0.1)\times10^{-35}$	$(0.448\pm0.07)\times10^{-35}$	$(0.246\pm0.16)\times10^{-35}$
4.5	$(1.60\pm0.2)\times10^{-35}$	$(1.46\pm0.2)\times10^{-35}$	$(0.692\pm0.28)\times10^{-35}$	
4.7	$(4.76\pm0.8)\times10^{-36}$	$(4.27\pm0.9)\times10^{-36}$	$(1.75\pm1.0)\times10^{-36}$	
4.9	$(1.87\pm0.5)\times10^{-36}$	$(3.48\pm0.7)\times10^{-36}$	$(1.02\pm0.5)\times10^{-36}$	

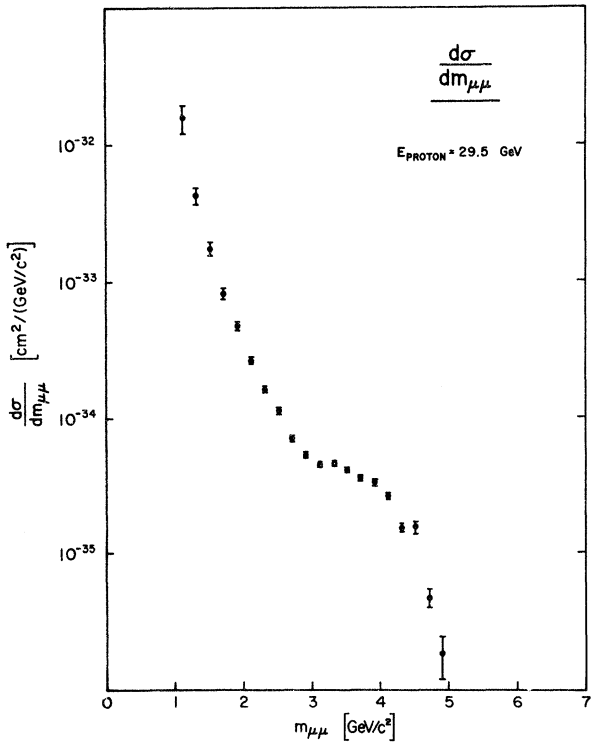

FIG. 6. $d\sigma/dm$. Proton energy = 29.5 GeV.

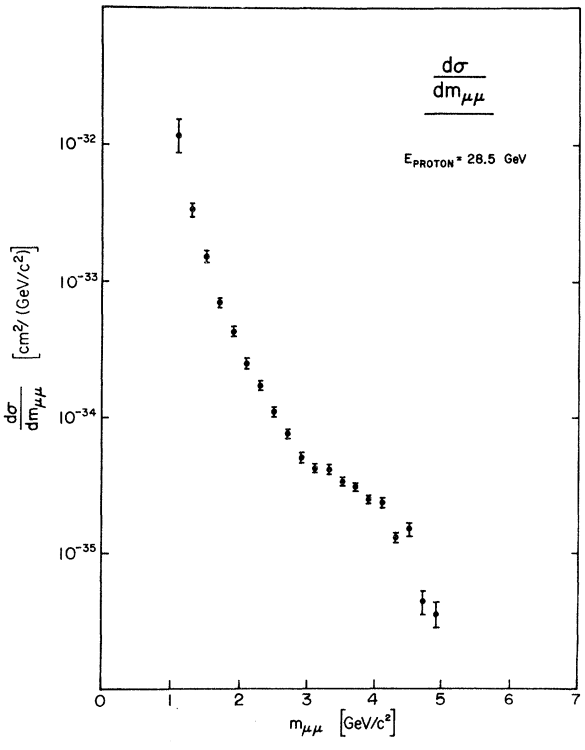

FIG. 7. $d\sigma/dm$. Proton energy = 28.5 GeV.

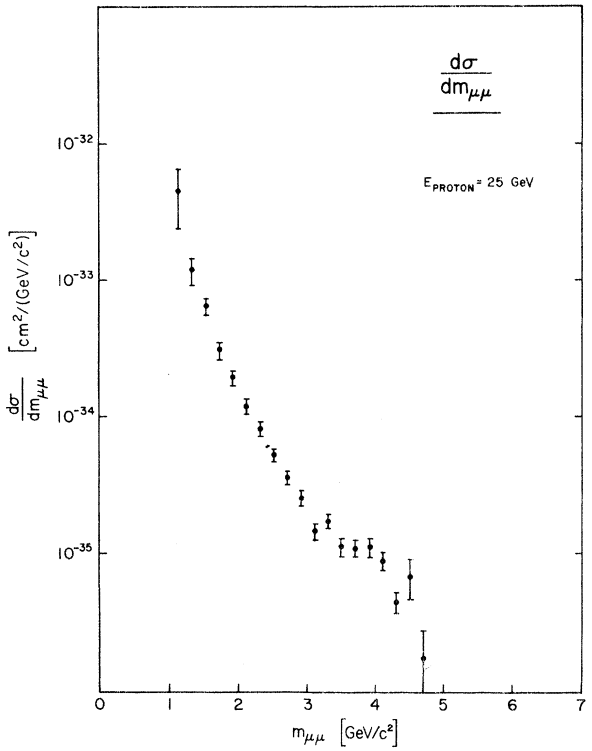

FIG. 8. $d\sigma/dm$. Proton energy = 25.0 GeV.

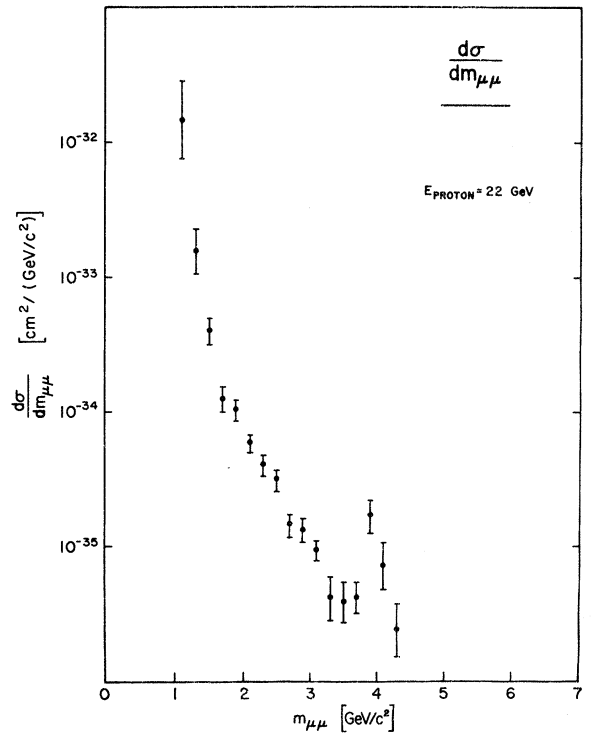

FIG. 9. $d\sigma/dm$. Proton energy = 22.0 GeV.

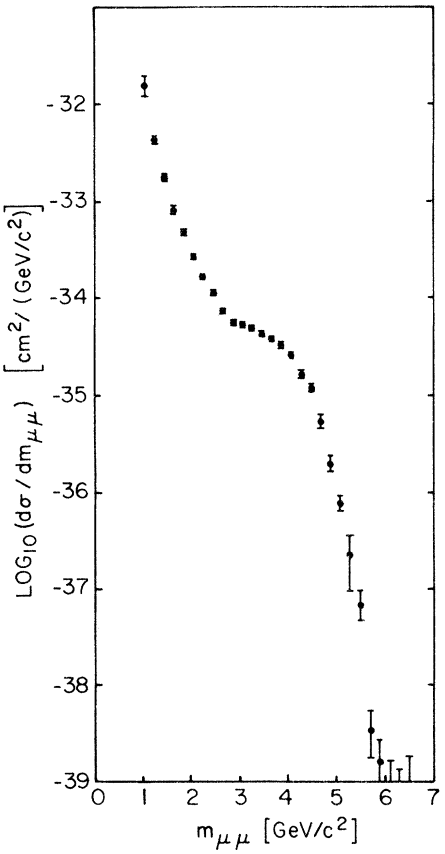

FIG. 10. $d\sigma/dm$. Weighted average of standard and "wide angle" events. Proton energy = 29.5 GeV.

every way analogous to the method used for the invariant mass. Tables III and IV give $d\sigma/dp_L$ and $d\sigma/d\cos\theta$ for all four incident energies, and Figs. 11 and 12 display $d\sigma/dp_L$ and $d\sigma/d\cos\theta$ respectively for an incident proton energy of 29.5 GeV. The cross-section differential in the laboratory momentum is seen to fall steeply above a momentum of about 15 GeV/c. The cross section shows a slow variation as a function of $\cos\theta$ ($\approx e^{-500(1-\cos\theta)}$) which amounts to only a factor of $1/e$ over the aperture surveyed.

Figure 13 shows the production cross section differential in the dimuon transverse momentum at a proton energy of 29.5 GeV. It is believed that the arrangement of the apparatus in this experiment resulted in a limited sensitivity to this variable, and, in particular, the distribution is influenced by the specific model chosen to represent the variables of more primary interest. Also the distribution is affected by the laboratory "aperture" (particularly the requirement that $P_{\text{lab}} \geq 12$ GeV/c), and, if this effect is removed, the cross section roughly indicates an $e^{-P_T/0.4}$ behavior.

The total cross sections, within the experimen-

TABLE II. $d\sigma/dm$ for $E_{\text{proton}}=29.5$ GeV.

Mass (GeV/c^2)	$\frac{d\sigma}{dm}$ [cm^2/(GeV/c^2)]	Random errors (%)	Systematic errors (%)
1.1	1.61×10^{-32}	24	65
1.3	4.37×10^{-33}	11	65
1.5	1.80×10^{-33}	8	60
1.7	8.38×10^{-34}	8	55
1.9	4.81×10^{-34}	5	45
2.1	2.66×10^{-34}	5	35
2.3	1.69×10^{-34}	5	30
2.5	1.14×10^{-34}	5	30
2.7	7.21×10^{-35}	5	30
2.9	5.60×10^{-35}	7	35
3.1	5.32×10^{-35}	7	35
3.3	4.90×10^{-35}	6	30
3.5	4.24×10^{-35}	6	30
3.7	3.86×10^{-35}	7	25
3.9	3.30×10^{-35}	6	25
4.1	2.55×10^{-35}	7	30
4.3	1.60×10^{-35}	7	30
4.5	1.17×10^{-35}	10	30
4.7	5.32×10^{-36}	17	35
4.9	1.95×10^{-36}	21	35
5.1	7.72×10^{-37}	18	35
5.3	2.24×10^{-37}	59	35
5.5	7.09×10^{-38}	34	50
5.7	3.52×10^{-39}	51	50
5.9	1.64×10^{-39}	67	65
6.1	8.58×10^{-40}	92	75
6.3	5.13×10^{-40}	161	80
6.5	8.73×10^{-40}	110	85
6.7	4.84×10^{-40}	97	90

tal aperture, were calculated for each proton energy considered and are shown in Fig. 14 and Table V. The total cross section increases by a factor of 5 as the proton kinetic energy rises from 22 GeV to 29.5 GeV. However, the relative influence of the aperture should be recalled. This graph is useful only to confront theoretical models after application of the apparatus cuts.

B. Cross-Section Uncertainties

1. *Statistical Errors*

The statistical errors shown on each point of the differential cross sections (Figs. 6–13) were obtained by combining in quadrature the statistical errors of the data and the Monte Carlo calculations.

TABLE III. $d\sigma/dp_{11}$ for four incident energies.

	$\frac{d\sigma}{dp_{11}}$ [cm^2/(GeV/c)]			
Longitudinal momentum (GeV/c)	E_{proton} 29 GeV	28.5 GeV	25 GeV	22 GeV
13	$(3.90\pm0.7)\times10^{-34}$	$(3.32\ \pm0.7)\times10^{-34}$	$(1.92\ \pm0.5\ )\times10^{-34}$	$(1.38\ \pm0.5\ )\times10^{-34}$
15	$(5.14\pm0.6)\times10^{-34}$	$(4.77\ \pm0.6)\times10^{-34}$	$(2.77\ \pm0.4\ )\times10^{-34}$	$(1.23\ \pm0.3\ )\times10^{-34}$
17	$(2.85\pm0.2)\times10^{-34}$	$(2.79\ \pm0.2)\times10^{-34}$	$(1.42\ \pm0.2\ )\times10^{-34}$	$(0.53\ \pm0.09)\times10^{-34}$
19	$(1.80\pm0.2)\times10^{-34}$	$(1.75\ \pm0.2)\times10^{-34}$	$(0.719\pm0.08\ )\times10^{-34}$	$(0.115\pm0.03)\times10^{-34}$
21	$(9.72\pm0.8)\times10^{-35}$	$(8.75\ \pm0.8)\times10^{-35}$	$(2.81\ \pm0.3\ )\times10^{-35}$	$(0.187\pm0.07)\times10^{-35}$
23	$(4.07\pm0.4)\times10^{-35}$	$(3.40\ \pm0.3)\times10^{-35}$	$(0.696\pm0.1\ )\times10^{-35}$	
25	$(1.60\pm0.2)\times10^{-35}$	$(1.30\ \pm0.1)\times10^{-35}$	$(0.026\pm0.007)\times10^{-35}$	
27	$(3.18\pm0.4)\times10^{-36}$	$(2.47\ \pm0.4)\times10^{-36}$		
29	$(1.33\pm0.2)\times10^{-37}$	$(0.819\pm0.2)\times10^{-37}$		

TABLE IV. $d\sigma/d\cos\theta$ for four incident energies.

	$10^{30}\frac{d\sigma}{d\cos\theta}$ (cm^2)			
	E_{proton}			
$\cos\theta$	29.5 GeV	28.5 GeV	25 GeV	22 GeV
1.0	2.27 ±0.1	1.94±0.1	0.871±0.06	0.44 ±0.03
0.9996	1.52 ±0.1	1.45±0.1	0.67 ±0.05	0.341±0.03
0.9992	1.33 ±0.1	1.18±0.1	0.526±0.05	0.287±0.05
0.9988	1.02 ±0.1	1.02±0.1	0.523±0.08	0.260±0.11
0.9984	0.989±0.2	1.08±0.2	0.696±0.14	0.276±0.13

2. *Systematic Errors*

The uncertainties in the subtraction procedure and in the effectiveness of the switching technique were calculated from the special runs in which both circuits were operared in the "delayed" mode. The error in the cross section determined by this method was estimated to be ±7½%. This uncertainty was included in the errors given in Fig. 14 for the total cross sections at each proton energy.

Further over-all uncertainties arise from the proton flux calculations (±20%), the choice of an approximate nucleon-nucleon inelastic cross section (±20%), the various physical assumptions involved in the Monte Carlo calculations (±35%), and lack of knowledge of the dimuon production distributions (±30%). The sensitivity of these results to these last two effects was easily established by appropriately varying the relevant parameters of

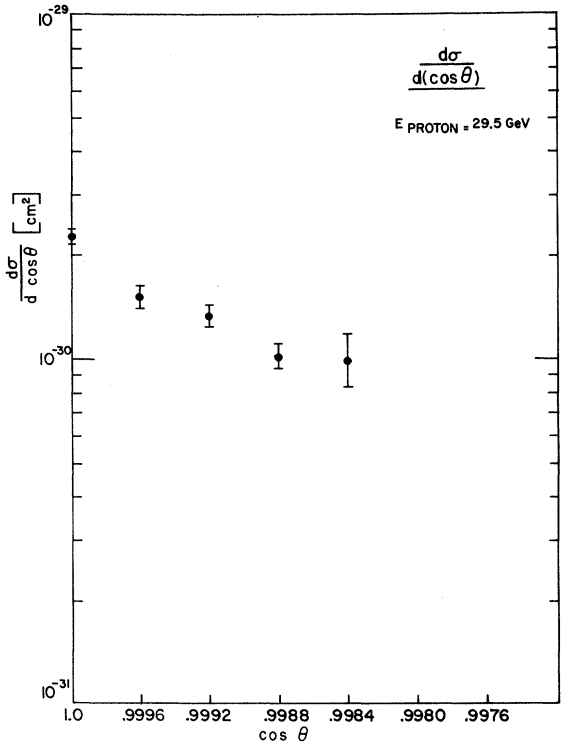

FIG. 12. $d\sigma/d\cos\theta$. Proton energy = 29.5 GeV.

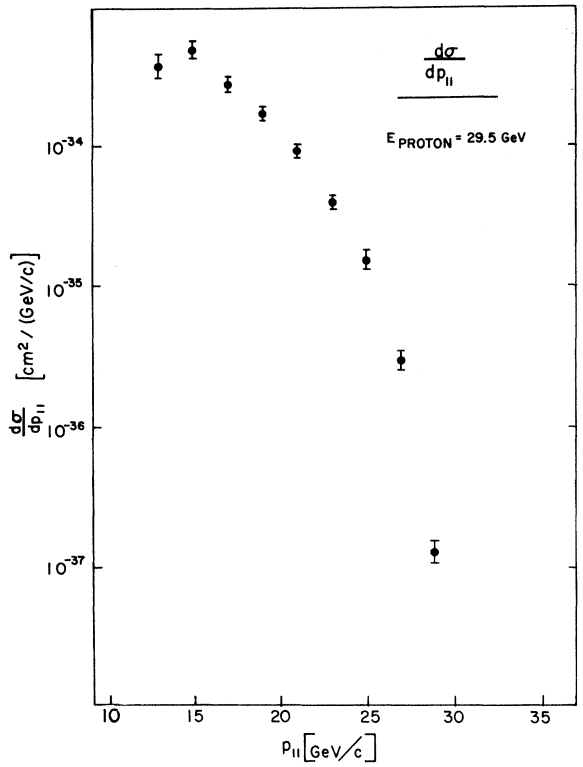

FIG. 11. $d\sigma/dp_{\parallel}$. Proton energy = 29.5 GeV.

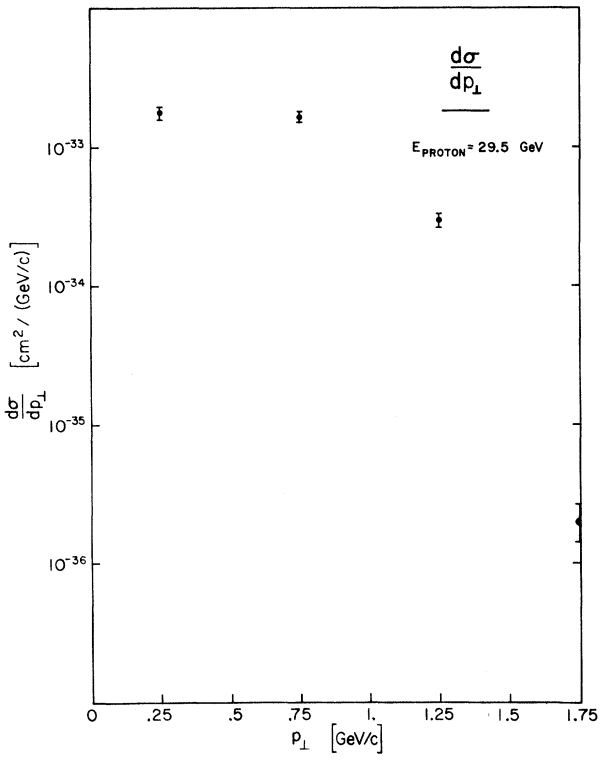

FIG. 13. $d\sigma/dp_{\perp}$. Proton energy = 29.5 GeV.

the Monte Carlo program and observing the output distributions. As previously mentioned, the distribution in θ_μ^*, the decay angle of the muon in the dimuon center of mass, was assumed to be isotropic. Monte Carlo studies show that distributions[30,31] such as $\sin^2\theta_\mu^*$ or $1+\cos^2\theta_\mu^*$ produce an over-all normalization uncertainty of ±20%. Of course, if this decay distribution were known independently, then the results of this experiment could be appropriately modified (cross sections reduced by 20% if the distribution were $\sin^2\theta_\mu^*$ or increased by 20% if the distribution were $1+\cos^2\theta_\mu^*$). In this case, the effect should not be included in the over-all uncertainty as it has been here.

In summary, uncertainties manifest themselves in four distinct ways: statistical errors on each point of a differential cross section, systematic model-dependent errors describing a "road" or "envelope" about the quoted cross section, systematic errors that can be assigned to the ordinate of the differential cross sections at any incident energy, and over-all systematic errors that are independent of energy. For convenience, the over-all errors described here have been folded in quadrature. For Figs. 6–14 this results in an uncertainty in the over-all normalization of ±60%.

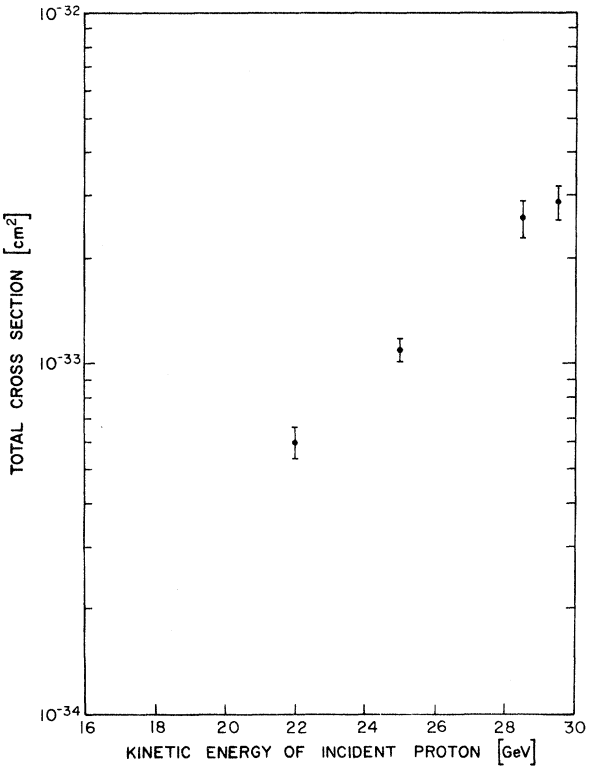

FIG. 14. Total cross section as a function of the energy of the incident proton.

V. DISCUSSION OF RESULTS

A. Nonobservation of Resonances

The invariant mass of the muon pair was the variable of primary interest for a simultaneous and, of course, highly related search made for "resonant" states. Any massive vector mesons would be expected to enhance the continuum near the resonance mass. As seen both in the observed mass spectrum (Fig. 4) and in the resultant cross sections $d\sigma/dq$ (Figs. 6–10) there is no forcing evidence of any resonant structure. However, to some extent, the smoothness of the cross section (for example, Fig. 10) is a reflection of the required smoothness of the input distribution to the Monte Carlo calculation. In order to properly investigate the production probability of a vector meson at a given mass, a narrow resonance was introduced into the Monte Carlo program, as an enhancement to a smooth continuum. The resonance was increased in amplitude until the resulting bump visibly distorted the output spectrum. This procedure properly introduced the single-particle mass resolution and efficiency into the analysis and enabled limits on vector-meson production to be calculated. The limits listed in Table VI represent the inseparable product of the production cross section of the vector particle and its branching ratio into two muons. It is noted that those limits apply to strong production of ρ-type particles as well as to production of neutral weak intermediate bosons.

The sensitivity to resonance production is clearly impaired by the rapidly falling continuum upon which any structure must reside. The precise shape of this nonresonant contribution is, of course, unknown. Figure 15 compares the experimentally observed mass spectrum with one based on a simple continuum of $1/m^5$ modified by three-body phase space. The choice of $1/m^5$ as a "reference" continuum was motivated by the fact that this simple power dependence seems successfully to fit the data for lower energies as well as being the mass dependence predicted by the vector-dominance model (see below). It is observed that for an incident proton energy of 29.5 GeV and for the

TABLE V. Total cross section for each incident kinetic energy.

Kinetic energy (GeV)	σ_{total} (cm^2)
29.5	$(2.9\pm0.3)\times10^{-33}$
28.5	$(2.6\pm0.3)\times10^{-33}$
25	$(1.2\pm0.1)\times10^{-33}$
22	$(6.0\pm0.6)\times10^{-34}$

mass range of 3–5 GeV/c^2, there is a distinct excess of the observed cross section over the reference curve. If this excess is assumed (certainly not required) to be the production of a resolution-broadened resonance, the cross-section–branching-ratio production σB would be approximately 6×10^{-35} cm^2, subject to the cross-section uncertainties discussed above. Alternatively the excess may be interpreted as merely a departure from the overly simplistic (and arbitrarily normalized) $1/m^5$ dependence. In this regard, we should remark that there may be two entirely different processes represented here: a low-Q^2 part which has to do with vector mesons, tail of the ρ, bremsstrahlung, etc., and a core yield with a slower mass dependence, which may be relevant to the scaling argument discussed below.

The "heavy photon" pole that has been postulated[32] to remove divergence difficulties in quantum electrodynamics would also be expected to contribute to the observed spectrum of muon pairs. This object (mass M_B) would modify the usual photon propagator by a multiplicative Breit-Wigner factor resulting in an integrated enhancement given by

$$\sigma_B = \frac{3\pi}{2\alpha} M_B \left(\frac{d\sigma}{dq}\right)_{q=M_B}. \tag{6}$$

Because this enhancement factor is strictly given by Eq. (6), this experiment sets a limit of 5 GeV/c^2 on the mass of the heavy photon.

B. The Continuum

1. General

This section considers several processes that could give rise to muon pairs. We make the fundamental assumption that what we have observed (or glimpsed) is the probability for the emission of a massive virtual photon in a close and complex hadronic collision. Standard models are considered. Some of these yield results too small to account for the observed cross sections. Other processes are open to several interpretations or formulations. Specific calculations have been made for several of these models.

A theoretical treatment of this process is complicated by the large number of secondary particles produced in the initial proton-uranium collision. In principle, these secondary particles could also create muon pairs. In this case, the observed spectrum would represent the inseparable product of the spectrum of the secondary particle and its own yield of muon pairs. In exploratory research of this kind this disadvantage is largely offset by the fact that the variety of initial states provides a more complete exploration of dimuon production in hadron collisions.

TABLE VI. Resonance limits as a function of mass.

Mass (GeV/c^2)	Resonance limits σB (cm^2)
1.5	2×10^{-32}
2.5	3×10^{-34}
3.5	3×10^{-34}
4.5	3×10^{-35}
5.5	4×10^{-35}

2. Real Photons

Real photons produced in the target (presumably from the decay of neutral pions) yield muon pairs by Bethe-Heitler or Compton processes. Estimates were made for the photon flux on the basis of pion-production models,[27,28] and this method of calculating the flux was checked against the experimental data of Fidecaro *et al.*[33] The argument was found to be within experimental uncertainties. The Bethe-Heitler cross section as calculated by Bjorken, Drell, and Frautschi[34] was evaluated for the kinematic region of this experiment. Calculations were made for complete coherence (i.e., production off the uranium nucleus) and also for

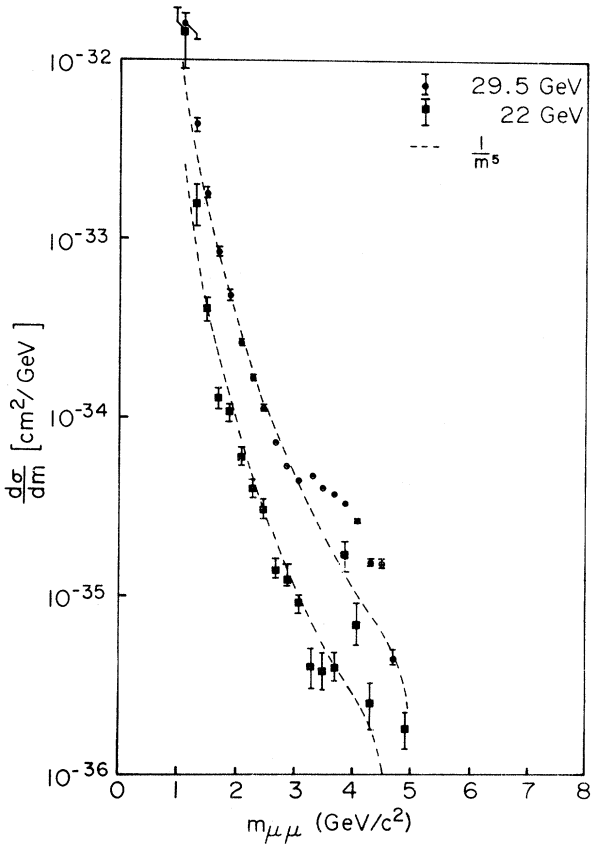

FIG. 15. Experimental cross sections at two energies compared with a simple $1/m^5$ continuum.

complete incoherence (individual nucleons). Estimates were also made of the effect of inelastic form factors at the nucleon vertex. In all cases the production of muon pairs by the Bethe-Heitler process was seen to be too small to contribute significantly to the observed signal.

3. *Virtual Photons*

The general formulation of the process of lepton pair production in nucleon-nucleon collisions was first considered by Oakes,[30] who expressed the cross section in terms of five form factors. One approach to the interpretation of the results of this experiment employs the ideas of vector dominance in which the interaction of the virtual photon with the hadrons is mediated by a vector meson. A calculation of Matveev *et al.*[35] has predicted the behavior of the observed muon pair continuum on the basis of the known vector mesons, ρ, ω, and ϕ. The calculation is partially phenomenological and suffers from a lack of available information on the production cross sections and characteristics of these vector mesons at high energies (~30 GeV). Nevertheless, the model does predict a mass dependence of $\approx 1/q^5$. The predicted curve is a factor of ~50 below the spectrum observed in this experiment (Fig. 10). No predictions of dimuon momentum or proton energy dependence are made. It has been suggested[31] that in the framework of the vector-dominance model, the decay distribution of the muon pair would be expected to vary as $\sin^2\theta_\mu^*$, indicating that the virtual (timelike) photon is longitudinally polarized.

The inelastic electron-proton scattering experiments[7] have prompted several theories. The concept of partons, or elementary constituent particles, has been introduced in the study of inelastic electron scattering,[36] and there have been suggestions that this kind of model is also capable of explaining processes involving timelike photons. Drell and Yan have postulated that the muon pairs observed in this experiment arise from a process of parton-antiparton annihilation.[37] This annihilation model, with certain functions measured in the spacelike region and some simplifying assumptions, is capable of predicting the salient features of the cross sections observed in this experiment. The model contains one free parameter, and the normalization of the model with respect to the data results in a prediction of $\lambda^2 \simeq 2$, where λ^2 is the square of the average charge of the individual parton. This model predicts that the virtual photon would be predominantly transversely polarized if it is formed by the annihilation of spin-$\frac{1}{2}$ parton-antiparton pairs. This would result in a muon-pair decay distribution of $1+\cos^2\theta_\mu^*$, in contrast to the predictions of vector dominance. Similar results have been obtained by Kuti and Weisskopf[38] and by Landshoff and Polkinghorne,[39] who use different variants of the parton annihilation model.

Also using analogies with the SLAC inelastic e-p scattering data, Berman, Levy, and Neff have constructed a model for the production of timelike muon pairs in hadron collisions.[40] A calculation was performed for the "elastic" process

$$p + N \to p + N + \mu^+ + \mu^- . \tag{7}$$

The model considered the radiation of the virtual photon by a massive elementary constituent of the nucleon (parton). This "parton-bremsstrahlung" model predicts an absolute yield that is too low by a factor of ~20 and falls too steeply with mass. In contrast, the laboratory momentum distribution does not exhibit the steep falloff with large momentum seen in the experimental cross section (Fig. 11).

A study by Altarelli, Brandt, and Preparata[41] also discusses muon pair production in hadron-hadron collisions. Restrictions arising from the SLAC scattering experiment and from Regge theory are incorporated in their model. The formulation here is in terms of the behavior of current products near the light cone. The resulting predictions contain two free parameters. The mass distribution expected on the basis of this model is in good agreement with the observed data. Altarelli *et al.* suggest that the polarization of the virtual photon would be a function of its mass and conclude that neither the completely longitudinal case nor the completely transverse case would dominate.

A rather spirited controversy has arisen as to the applicability of the light-cone theory to this reaction. This is discussed by Drell,[42] Jaffe,[43] Baker, Lu and Shrauner,[44] Preparata,[45] Bjorken,[46] and doubtless many others. These points of view may be resolved when lepton pair experiments are carried out at very large values of s, in the new CERN Intersecting Storage Rings (ISR) and National Accelerator Laboratory (NAL) accelerators.

The emphasis of the relevance of dilepton production on the spacetime structure of the product of currents is given by Cornwall[47] and by Abarbanel and Kogut.[48] A similar analysis is presented in a recent paper by Etim, Greco, and Srivastava.[49] A Regge theory which does not employ light-cone analysis (or partons or vector dominance) is given by Galfi and Kögerler.[50] Finally, possible contributions to this reaction from two photon terms has been given by Budnev,[51] by Fujikawa,[52] and by Carimalo, Parisi, and Kessler.[53] This process is entirely negligible at BNL energies but could

contribute significantly for low masses and very high s, i.e., at the ISR or at NAL.

4. $\bar{p}p \to \mu^+ + \mu^- + Anything$

As previously mentioned, the production of secondary particles in the uranium nucleus, while complicating the analysis of the experiment, permits a more complete survey of dimuon production. For example, antinucleons produced in the initial proton collisions should be able to annihilate with target nucleons to form muon pairs. The cross section for the reaction $\bar{p}p \to \bar{\mu}\mu$ can be written

$$\frac{d\sigma}{d\Omega} = \frac{\alpha^2}{16}\frac{1}{EP}\left[G_M{}^2(1+\cos^2\theta) + \left(\frac{M_p}{E}\right)^2 G_E{}^2 \sin^2\theta \right], \tag{8}$$

where G_M and G_E are the form factors of the proton, E and P are the energy and momentum of the incident $\bar{p}$ in the center of mass, and θ is the angle between the $\bar{\mu}$ and the $\bar{p}$ in the center-of-mass system. A special Monte Carlo program was written to calculate the efficiency of the apparatus for detecting such muon pairs. Antiprotons were produced with a momentum spectrum given by the theoretical curves of Sanford and Wang[27] (excellent agreement is shown with the beam survey data of Dekkers *et al.*[54]). The number of antiprotons produced with laboratory momentum >12 GeV/c was estimated to be 1.5×10^{-5} per incident proton. The antiprotons were allowed to annihilate into muon pairs according to the distribution of Eq. (8). Separate calculations were made for the extreme cases $G_M=1$, $G_E=0$; $G_M=0$, $G_E=1$; and $G_M=G_E=1$. The distribution of muon pairs was such that they would have tended to populate the special wide-angle counters shown in Fig. 1. An upper limit to the contribution to the observed signal from antiproton-proton annihilation was obtained by assuming that all muon pairs detected in these wide-angle counters originated from this source. These calculations, of course, ignore the observed dimuon continuum (presumably due to $pN \to pN + \mu\bar{\mu}$). A differential cross section was calculated, and, using estimates of statistical and systematic uncertainties, the limits for $\bar{p}p \to \bar{\mu}\mu$ shown in Fig. 16 were obtained (95% confidence level). Also shown are the limits obtained by the direct measurements of Refs. 17 and 18.

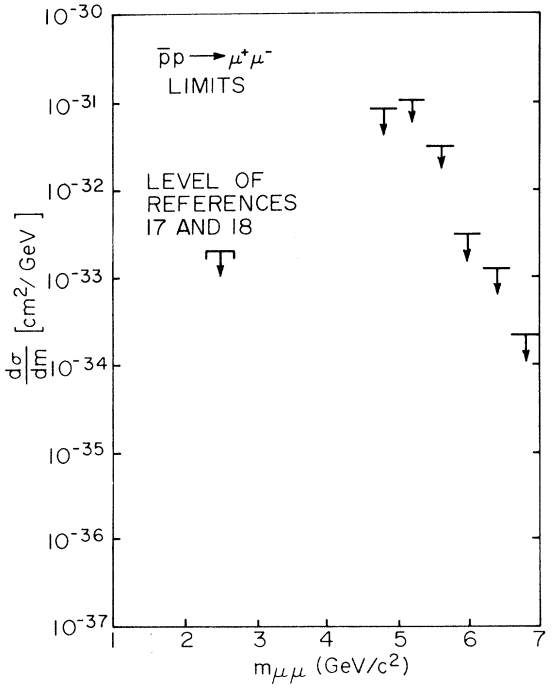

FIG. 16. Upper limits as a function of dimuon mass for the reaction $\bar{p}p \to \mu^+\mu^-$.

VI. IMPLICATIONS

A. CVC and Weak Interactions

This experiment evolved from a search for single muons at large P_T (Ref. 55) and the subsequent remark by Yamaguchi[56] that conservation of vector current (CVC) provides a relation between weak and electromagnetic processes which produce leptons in proton-proton collisions. Thus this experiment measures the flux of virtual photons emitted in a hadron-hadron collision, complete with whatever form factors beset these particles. CVC teaches us how to convert this amplitude into one for producing $W^{\pm}$ with subsequent decay into lepton pairs; $e\nu$, $\mu\nu$. These ideas have been applied[57] to

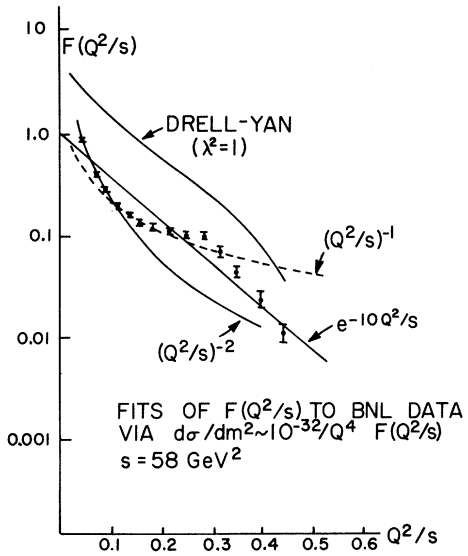

FIG. 17. $F(Q^2/s)$ shown for the experimental data, and various models.

set a limit on the mass of the W on the basis of cross-section limits for the yield of decay muons.[58]

B. Esoteric Particle Production

Given the experimental flux of virtual photons provided here, one can predict the production, at the same energy, of a variety of particles known to be coupled to virtual photons. Sculli and White[59] have carried this out for electromagnetic pair production of quarks and, via a small extrapolation to Serpukhov energy, have converted a cross-section limit obtained there to a mass limit $M_Q > 3$ GeV/c^2. In the same vein, Newmeyer and Trefil[60] have applied these results to a calculation of the production of magnetic monopoles via virtual photons. They establish a limit of $M > 5$ GeV from unsuccessful searches for accelerator-produced monopoles.

A similar analysis for the production of charged intermediate bosons,[57] $W^{\pm}$, enabled one to state a "plausible" mass limit of $M_W > 4$ GeV from accelerator searches for $W^{\pm}$, using CVC-type arguments to convert virtual photon flux to real $W^{\pm}$ flux.

The scaling theories briefly discussed above can be used to make predictions as to the yield of dileptons and therefore virtual photons for the new accelerators. In particular, a dimensional argument based on the assumption that the BNL data (similar to the SLAC data on e-p scattering) are in the scaling region permits one to produce curves of expected yields of dileptons, heavy leptons, magnetic monopoles, quarks, W's, B's, etc.[61] Experiments under way at the ISR and at NAL may soon establish the validity of any of these extrapolations.

VII. SUMMARY AND CONCLUSIONS

(1) A continuum yield of lepton pairs measures the flux of virtual photons in proton-nuclear collisions near 30 GeV. These results may be fitted with a simple expression of the form

$$\frac{d\sigma}{dq} = \frac{\alpha^2}{q^3} F\left(\frac{q^2}{s}\right), \quad q = M_{\mu\mu} \tag{9}$$

where $s \cong 60$ GeV^2 at BNL and $\alpha^2 = (\frac{1}{137})^2 = 2 \times 10^{-32}$ cm^2 GeV^2.

The form we have chosen here is motivated by popular scaling arguments. Note that the structure function is dimensionless.

We find $F(q^2/s) = e^{-10q^2/s}$ provides an acceptable fit for $0.1 \leq q^2/s \leq 0.5$, although simple power law, e.g., $F = 0.02s/q^2$, also "fits" (see Fig. 17). Although the form chosen implies a scaling regime, we stress that our range of s variation was too small and too sensitive to aperture to verify scaling.

(2) No resonances (i.e., 1^- bumps) are observed, and limits are given in Table VI.

(3) The transverse momentum of the dilepton falls off more slowly than typical hadronic emission.

(4) The dilepton longitudinal momentum distribution falls steeply with momentum. The behavior in the interesting region near zero is not well observed.

(5) Many of the theories which fit the deeply inelastic e-p scattering also give a good account of the data presented here. Only future experiments with much higher values of s and q^2 will decide which, if any, are correct.

ACKNOWLEDGMENTS

We would like to express an indebtedness to the staff of Nevis Laboratory who built and serviced the apparatus, in particular to William Sippach, who designed the electronics; to the staff of the On-Line Data Facility at Brookhaven who were essential to the smooth accumulation of data; to the staff of the then-fledgling slow external proton beam, especially Woody Glenn and our liaison engineer, Jack Detweiler; and to the numerous helpful discussions with both theorists and experimentalists at Columbia University and at Brookhaven.

---

*Research supported by the U. S. Atomic Energy Commission.

†Present address: New York University, New York, N. Y.

‡Present address: Northwestern University, Evanston, Illinois.

§Present address: CERN, Geneva, Switzerland.

[1]An abbreviated summary of this experiment has been published [Phys. Rev. Lett. 25, 1523 (1970)]. See also B. G. Pope, Ph.D. thesis, Columbia University, Nevis Report No. 185, 1970 (unpublished).

[2]R. Hofstadter, in *Electron Scattering and Nuclear and Nucleon Scattering*, edited by R. Hofstadter (Benjamin, New York, 1963).

[3]R. R. Wilson, Annu. Rev. Nucl. Sci. 14, 347 (1964).

[4]D. H. Coward, H. DeStaebler, R. A. Early, J. Litt, A. Minten, L. W. Mo, W. K. H. Panofsky, R. E. Taylor, M. Breidenbach, J. I. Friedman, H. W. Kendall, P. N. Kirk, B. C. Barish, J. Mar, and J. Pine, Phys. Rev. Lett. 20, 292 (1968).

[5]Y. Nambu, Phys. Rev. 106, 1366 (1957).

[6]For example: W. R. Frazer and J. R. Fulco, Phys. Rev. 117, 1609 (1960); M. Gell-Mann and F. Zachariasen, *ibid.* 124, 953 (1961). A good review is given by J. J. Sakurai, in *Lectures in Theoretical Physics*, edited by W. E. Brittin *et al.* (Gordon and Breach, New York,

1968), Vol. XI.

[7]J. R. Dunning, K. W. Chen, A. A. Cone, G. Hartwig, N. F. Ramsey, J. K. Walker, and R. Wilson, Phys. Rev. Lett. 13, 631 (1964); M. Goitein, J. R. Dunning, and R. Wilson, *ibid.* 18, 1018 (1967).

[8]E. D. Bloom, D. H. Coward, H. DeStaebler, J. Drees, G. Miller, L. W. Mo, R. E. Taylor, M. Breidenbach, J. I. Friedman, G. C. Hartmann, and H. W. Kendall, Phys. Rev. Lett. 23, 930 (1969); M. Breidenbach, J. I. Friedman, H. W. Kendall, E. D. Bloom, D. H. Coward, H. De Staebler, J. Drees, L. W. Mo, and R. E. Taylor, *ibid.* 23, 935 (1969).

[9]R. P. Feynman, Phys. Rev. Lett. 23, 1415 (1969).

[10]J. E. Augustin, J. Buon, B. Delcourt, J. Jeanjean, D. Lalanne, H. Nguyen Ngoc, J. Perez-y-Jorba, P. Petroff, F. Richard, F. Rumpf, and D. Treille, Phys. Lett. 31B, 673 (1970).

[11]J. J. Russell, R. C. Sah, M. J. Tannenbaum, W. E. Cleland, D. G. Ryan, and D. G. Stairs, Phys. Rev. Lett. 26, 46 (1971).

[12]D. R. Earles, R. C. Chase, W. L. Faissler, M. W. Gettner, G. Glass, G. Lutz, R. G. Parsons, P. L. Rothwell, K. M. Moy, H. von Briesen, E. von Goeler, and R. Weinstein, Phys. Rev. Lett. 25, 129 (1970).

[13]J. Bailey, W. Bartl, G. von Bochmann, R. C. A. Brown, F. J. M. Farley, H. Jostlein, E. Picasso and R. W. Williams, Phys. Lett. 28B, 287 (1968).

[14]Large amounts of experimental data are reviewed by S. C. C. Ting, in *Proceedings of the Fourteenth International Conference on High Energy Physics, Vienna, 1968,* edited by J. Prentki and J. Steinberger (CERN, Geneva, 1968). Data include P. L. Rothwell, R. C. Chase, D. R. Earles, M. Gettner, G. Glass, G. Lutz, E. von Goeler, and R. Weinstein, Phys. Rev. Lett. 23, 1521 (1969); G. McClellan, N. Mistry, P. Mostek, H. Ogren, A. Osborne, A. Silverman, J. Swartz, R. Talman, and G. Diambrini-Palazzi, *ibid.* 23, 554 (1969).

[15]J. E. Augustin, J. C. Bizot, J. Buon, J. Haissinski, D. Lalanne, P. Marin, H. Nguyen Ngoc, J. Perez-y-Jorba, F. Rumpf, E. Silva, and S. Tavernier, Phys. Lett. 28B, 508 (1969); V. L. Auslander, G. I. Budker, Ju. N. Pestov, V. A. Siderov, A. N. Skrinsky, and A. G. Khabakhpashev, *ibid.* 25B, 433 (1967).

[16]The following investigations have revealed no evidence for heavy mesons coupling to lepton pairs up to masses of 2.1 GeV/c^2: G. McClellan, N. Mistry, P. Mostek, H. Ogren, A. Osborne, A. Silverman, J. Swartz, R. Talman, and G. Diambrini-Palazzi, Phys. Rev. Lett. 23, 718 (1969); S. Hayes, R. Imlay, P. M. Joseph, A. S. Keizer, J. Knowles and P. C. Stein, Phys. Rev. Lett. 24, 1369 (1970); D. R. Earles, W. L. Faissler, M. Gettner, G. Lutz, K. M. Moy, Y. W. Tang, H. von Briesen, E. von Goeler, and R. Weinstein, *ibid.* 25, 1312 (1970).

[17]M. Conversi, T. Massam, Th. Muller, and A. Zichichi, Nuovo Cimento 40, 690 (1965). B. Barish, D. Fong, R. Gomez, D. Hartill, J. Pine, A. V. Tollestrup, A. Maschke, and T. Zipf, Caltech Report No. CALT-68-70, 1966 (unpublished).

[18]B. Bartoli, F. Felicetti, H. Ogren, V. Silvestrini, G. Marini, A. Nigro, and F. Vanoli, Phys. Rev. D 6, 2374 (1973).

[19]A. Wehmann, E. Engels, L. N. Hand, C. M. Hoffman, P. G. Innocenti, R. Wilson, W. A. Blanpied, D. J. Drickey, and D. G. Stairs, Phys. Rev. 178, 2095 (1969).

[20]B. D. Hyams, W. Koch, D. Pellett, D. Potter, L. von Lindern, E. Lorenz, G. Lutgens, U. Stierlin, and P. Weilhammer, Phys. Lett. 24B, 634 (1967).

[21]M. N. Khachaturyan, M. A. Azimov, A. M. Baldin, A. S. Belousov, I. V. Chuvilo, R. Firkowski, J. Hladky, M. S. Khvastunov, J. Manca, A. T. Matyushin, V. T. Matyushin, G. A. Ososkov, L. N. Shtarkov, and L. I. Zhuravleva, Phys. Lett. 24B, 349 (1967).

[22]J. D. Fox, G. W. Bennett, G. S. Levine, R. J. Nawrocky, L. E. Repeta, and A. V. Soukas, in *Proceedings of the 1969 Particle Accelerator Conference,* Washington, p. 832.

[23]J. Geibel, K. H. Reich, J. Seetzen, A. Citron, L. Hoffman, C. Passow, W. R. Nelson, M. Whitehead, R. L. Childers, C. D. Zerby, C. M. Fisher, R. H. Thomas, J. Baarli, K. Goebel, A. H. Sullivan, and J. Ranft, Nucl. Instrum. Methods 32, 45 (1965). A study was made of the development of the nuclear cascade initiated in steel by primary protons of 10 and 20 GeV.

[24]E. Fermi, as quoted by B. Rossi, *High Energy Particles* (Prentice-Hall, Englewood Cliffs, N. J., 1956), p. 71.

[25]R. M. Sternheimer, Phys. Rev. 115, 137 (1959); P. M. Joseph, Cornell University Report No. CLNS-52, 1969 (unpublished).

[26]R. M. Sternheimer, Phys. Rev. 117, 485 (1960).

[27]J. R. Sanford and C. L. Wang, BNL report, 1967 (unpublished); C. L. Wang, Phys. Rev. Lett. 25, 1068 (1970).

[28]Other pion production formulas and experimental references are given by J. W. Rettberg [Ph.D. thesis, Columbia University, Nevis Report No. 152, 1966 (unpublished)] and by R. Hagedorn and J. Ranft [Nuovo Cimento Suppl. 6, 169 (1968)].

[29]E. W. Anderson, E. J. Bleser, G. B. Collins, T. Fujii, J. Menes, F. Turkot, R. A. Carrigan, R. M. Edelstein, N. C. Hien, T. J. McMahon, and I. Nadelhaft, Phys. Rev. Lett. 19, 198 (1967). The cross section was chosen to represent the probability of the proton engaging in any nuclear interaction (cross section 38 mb) while ignoring those processes that were elastic or so close to elastic (say an energy loss < 5 GeV) that the emergent proton was still capable of dimuon production.

[30]R. J. Oakes, Nuovo Cimento 44A, 440 (1966).

[31]J. J. Sakurai, Phys. Rev. Lett. 24, 968 (1970).

[32]T. D. Lee and G. C. Wick, Phys. Rev. D 2, 1033 (1970).

[33]M. Fidecaro, G. Gatti, G. Giacomelli, W. A. Love, W. C. Middelkoop, and T. Yamagata, Nuovo Cimento 19, 382 (1961).

[34]J. D. Bjorken, S. D. Drell, and S. C. Frautschi, Phys. Rev. 112, 1409 (1958).

[35]V. A. Matveev, R. M. Muradyan, and A. N. Tavkhelidze, JINR Dubna report, 1969 (unpublished); M. Mestvivishrili, Serpukhov Report No. IHEP-STF-70-46, 1970 (unpublished).

[36]R. P. Feynman, quoted by J. D. Bjorken, SLAC Report No. SLAC-PUB-571, 1969 (unpublished). See also Ref. 8.

[37]S. D. Drell and T.-M. Yan, Phys. Rev. Lett. 25, 316 (1970).

[38]J. Kuti and V. F. Weisskopf, Phys. Rev. D 4, 3418 (1971).

[39]P. V. Landshoff and J. C. Polkinghorne, Nucl. Phys. B33, 221 (1971); B36, 642(E) (1972); Cambridge

University Report No. DAMTP 72-10, 1972 (unpublished).
[40]S. M. Berman, D. J. Levy, and T. L. Neff, Phys. Rev. Lett. 23, 1363 (1969).
[41]G. Altarelli, R. A. Brandt, and G. Preparata, Phys. Rev. Lett. 26, 42 (1971); R. A. Brandt and G. Preparata, Phys. Rev. D 6, 619 (1972); R. A. Brandt, 1972 Erice lectures, CERN Report No. TH 1557 (unpublished).
[42]S. D. Drell and T.-M. Yan, Ann. Phys. (N.Y.) 66, 578 (1971).
[43]R. L. Jaffe, Phys. Rev. D 5, 2622 (1972).
[44]H. C. Baker, E. Y. C. Lu, and E. Shrauner, Phys. Lett. 38B, 110 (1972).
[45]G. Preparata, BNL Report No. 16173, 1971 (unpublished).
[46]J. D. Bjorken, rapporteurs' talk, in *Proceedings of the International Symposium on Electron and Photon Interactions at High Energy, 1971,* edited by N. B. Mistry (Laboratory of Nuclear Studies, Cornell Univ., Ithaca, N. Y., 1972).
[47]J. Cornwall, Phys. Rev. D 5, 2863 (1972).
[48]H. D. I. Abarbanel and J. B. Kogut, Phys. Rev. D 5, 2050 (1972).
[49]E. Etim, M. Greco, and Y. N. Srivastava, CNEN Frascati Report No. 72-65, 1972 (unpublished).
[50]L. Galfi and R. Kögerler, Phys. Lett. 36B, 218 (1971).
[51]V. M. Budnev, I. F. Ginzburg, G. V. Meledin, and V. G. Serbo, Zh. Eskp. Teor. Fiz. Pis'ma Red. 12, 349 (1970) [JETP Lett. 12, 238 (1970)].
[52]K. Fujikawa, Nuovo Cimento 12B, 117 (1972).
[53]C. Carimalo, J. Parisi, and P. Kessler (unpublished).
[54]D. Dekkers, J. A. Geibel, R. Mermod, G. Weber, T. R. Willitts, K. Winter, B. Jordan, M. Vivargent, N. M. King, and E. J. N. Wilson, Phys. Rev. 137, B962 (1965).
[55]R. Burns, G. Danby, E. Hyman, L. M. Lederman, W. Lee, J. Rettberg, and J. Sunderland, Phys. Rev. Lett. 15, 830 (1965).
[56]Y. Yamaguchi, Nuovo Cimento 43A, 193 (1966).
[57]L. M. Lederman and B. G. Pope, Phys. Rev. Lett. 27, 765 (1971).
[58]P. J. Wanderer, R. J. Stefanski, R. K. Adair, C. M. Ankenbrandt, H. Kasha, R. C. Larsen, L. B. Leipuner, and L. W. Smith, Phys. Rev. Lett. 23, 729 (1969).
[59]J. Sculli and T. O. White, Phys. Rev. Lett. 27, 619 (1971).
[60]J. L. Newmeyer and J. S. Trefil, Phys. Rev. Lett. 26, 1509 (1971).
[61]L. M. Lederman (unpublished).

PHYSICAL REVIEW D VOLUME 8, NUMBER 7 1 OCTOBER 1973

Transverse-Momentum–Correlation Features in Multipion Annihilations at 5.7 GeV/c

H. Braun, A. Fridman, J.-P. Gerber, P. Juillot, J. A. Malko, G. Maurer, A. Michalon, and M. E. Michalon-Mentzer
Laboratoire de Physique Corpusculaire, Centre de Recherches Nucléaires de Strasbourg, Rue du Loess, Strasbourg, Cronenbourg, France
(Received 10 January 1973)

A study of the two-particle correlation in the $\bar{p}p \to 3\pi^+3\pi^-$, $\bar{p}p \to 3\pi^+3\pi^-\pi^0$, $\bar{p}p \to 4\pi^+4\pi^-$, and $\bar{p}p \to 4\pi^+4\pi^-\pi^0$ reactions was carried out by means of variables constructed from $\vec{r}_1$ and $\vec{r}_2$, the transverse momenta of the particles entering in each considered pair of pions. We show that transverse-momentum–correlation information can be obtained by using the convenient variables $P^2 = |\vec{r}_1 + \vec{r}_2|^2$ and $Q^2 = |\vec{r}_1 - \vec{r}_2|^2$. The fourth differential distribution $d^4N/(d\vec{r}_1 d\vec{r}_2)$ was described by a simple parametrization allowing a direct measurement of the transverse-momentum correlation for the $\pi^\pm\pi^\pm$ and $\pi^+\pi^-$ pairs.

I. INTRODUCTION

The numerous investigations carried out recently on inclusive processes have stimulated new studies on the two-particle correlation. In the present work we will study the two-particle correlation in multipion $\bar{p}p$ annihilation at 5.7 GeV/c using for this purpose new two-particle variables. The reactions which we consider are

$$\bar{p}p \to 3\pi^+3\pi^- \quad (1)$$
$$\to 3\pi^+3\pi^-\pi^0 \quad (2)$$
$$\to 4\pi^+4\pi^- \quad (3)$$
$$\to 4\pi^+4\pi^-\pi^0 . \quad (4)$$

Details on the experimental procedure and on the general production features of the $\bar{p}p \to 6\pi, 7\pi$ reactions can be found in Ref. 1, in which about $\frac{1}{5}$ of the present data were handled. Some results on the $\bar{p}p \to 8\pi, 9\pi$ channels have already been published.[2] The numbers of events used for the present analysis and which belong to the channels (1) through (4) are 667, 2413, 107, and 246, respectively.

One difficulty in investigating the two-particle correlation consists in the choice of variables. Recent works have shown[3-6] that the study of correlation between transverse momenta may be useful for testing various theoretical models. Follow-